Received: 26 March 2022 | Revised: 7 September 2022 | Accepted: 21 September 2022

DOI: 10.1111/ffe.13853

ORIGINAL ARTICLE

FFEMS Fatigue & Fracture of Engineering Materials & Structures WILEY

Sensitivity and uncertainty analysis for structural health monitoring with crack propagation under random loads: A numerical framework in the frequency domain

Denys Marques[1] | **Dirk Vandepitte**[2] | **Volnei Tita**[1,3]

[1]Aeronautical Engineering Department, São Carlos School of Engineering, University of São Paulo, São Carlos, Brazil

[2]Department of Mechanical Engineering, KU Leuven, Leuven, Belgium

[3]Department of Mechanical Engineering, Faculty of Engineering of University of Porto, Porto, Portugal

Correspondence
Denys Marques, Aeronautical Engineering Department, São Carlos School of Engineering, University of São Paulo, São Carlos, SP, Brazil.
Email: denys.marques@usp.br

Funding information
National Council for Scientific and Technological Development, Grant/Award Number: 310656/2018-4; Coordenação de Aperfeiçoamento de Pessoal de Nível Superior—Brasil (CAPES), Grant/Award Number: Finance Code 001

Abstract

The quantification of uncertainties in a system and the ability to identify the most influential parameters for a given structural health monitoring (SHM) strategy constitutes an important step for an in-depth analysis of the problem. It is used in reliability assessment and for the definition of proper inspection intervals. In a recent paper, the authors proposed a methodology for SHM and fatigue life estimations of structures under random loads. This paper expands over those concepts and presents a framework for sensitivity and uncertainty analysis for SHM of structures in the frequency domain. The structure is an Euler–Bernoulli beam, which is modeled with the Ritz method. The conceptual simplicity of the Ritz model keeps the computational cost low. The results showed that the Walker parameter for the crack propagation law, C_0; the modal damping factor; and the input acceleration are important parameters affecting the variance of the remaining useful life.

KEYWORDS

fatigue, global sensitivity analysis, random loads, structural health monitoring, uncertainty propagation

1 | INTRODUCTION

Fatigue failure is one of the main concerns in the design of structures in several branches of industry, such as aeronautics. Different design philosophies have been developed to prevent this type of failure, namely, safe-life, fail-safe, and damage-tolerant. The damage-tolerant approach, in particular, is commonly applied in the aeronautical industry, allowing weight savings while at the same time ensuring structural reliability.[1] This design methodology tolerates small cracks to propagate without jeopardizing structural safety. It does rely heavily on non-destructive inspection techniques and proper inspection intervals and maintenance plans.

Structural health monitoring (SHM) systems are a natural complement to the damage-tolerant philosophy, as they are based on methods for the non-destructive monitoring of the damage state of a structure, with the final objective of a complete condition-based maintenance that is autonomous and continuous.[2] Vibration-based methods are successfully applied in SHM systems.[3–6] Since these methods rely on monitoring changes in the dynamic response, they should be able to cope with the inherent variability of structures (in terms of their geometric characteristics and material properties) and still unequivocally identify the presence of damage. Moreover, the quantification of uncertainties in a system and the ability to identify the dominant parameters for a given SHM strategy constitutes an important step for an in-depth analysis of the problem.

According to Datteo et al.,[7] uncertainty propagation is the process of quantifying the uncertainty in the result of

a function based on the uncertainty of its inputs. This process usually requires a very large number of evaluations of a mathematical model, which can be computationally intensive. When the model gets too large, a surrogate model (SM) brings down the computation time. Common methods for generating a SM are polynomial chaos expansion, Kriging, ANOVA decomposition, and neural networks.[7]

In recent years, much research effort is spent on modeling uncertainty and reliability of metallic structures subjected to fatigue damage. Marques et al.[8] evaluated the reliability of a riveted railway bridge using Monte Carlo simulations. Crack propagation was modeled using the standard Paris crack propagation model and considering as statistical properties the Paris coefficient C and exponent m, the stress range, and the initial and critical crack lengths. They concluded that the annual traffic growth rate is a very important parameter that affects structural fatigue life. Datteo et al.[7] implemented an autoregressive model in a 1 degree-of-freedom system subjected to a Gaussian white noise excitation. They use a damage feature based on the Mahalanobis' squared distance (MSD) to study the sensitivity and uncertainty analysis of this model technique in the context of SHM using a global sensitivity analysis (GSA) based on Sobol's indices. They showed that the MSD as a damage feature is more sensitive to changes in natural frequencies than to changes in damping ratio, indicating that it would not be a suitable parameter for damage cases that are expected to cause large variation in damping with small changes in natural frequencies of a structure.

Kala[9] used GSA to study the probability of failure of a steel bridge. Crack propagation was modeled using linear fracture mechanics. The results of the probability analysis were updated with results from bridge inspections of the presence of fatigue cracks and a methodology for optimal inspection times is devised. The stress range was identified as the dominant random variable by the sensitivity analysis.

Chen et al.[10] present an online updating Gaussian Process measurement model for fatigue crack prognosis. Crack prognosis is achieved using a particle filter-based framework in which an SHM measurement is used as input for the model and the NASGRO equation for crack growth is then randomized and used to model crack growth. The authors verified their method in attachment lug specimens under constant amplitude loads and they showed that with the updating procedure the relative error in the prognostic for the failure cycle was below 3% after 20,000 cycles.

Sankararaman et al.[11] proposed a methodology for uncertainty quantification (UQ) and model validation of fatigue crack growth. Their analysis includes uncertainty from natural variability in loading and material properties, data uncertainty, and modeling uncertainty, which are connected through a Bayesian network. To reduce the computational cost, the authors replace a finite element model for the calculation of the equivalent stress intensity factor (SIF) with a SM, and GSA is used to quantify the influence of each source of uncertainty.

Leser et al.[12] also proposed a general methodology for fatigue damage prognosis using SMs. SIFs for a 3D geometry are obtained from high-fidelity numerical models, and the data are used to train the SM, thus reducing the computational cost, while crack propagation is evaluated using the Walker equation. Furthermore, they include information from an SHM system, along with the Bayes inverse theorem, to obtain the posterior density distribution of the model random variables. The final result is a probabilistic prediction of the remaining useful life (RUL) of the structure of interest.

Recently, the present authors proposed a methodology in the frequency domain for SHM and fatigue life estimations of structures under random loads.[13] The structure investigated in Marques et al.[13] is a cantilever beam with a tip mass, which is a very useful model to be used as a first approximation for the behavior of many real-world structures, such as for the conceptual design of an airplane wing, a wind turbine blade or even a wind tower itself. Nevertheless, the large number of model evaluations required for the sensitivity and uncertainty analysis can make the use of complex models, such as the ones developed in finite elements, prohibitive even for this type of structure. In the present work, this issue is overcome by modeling the structure with the Ritz method for an Euler–Bernoulli beam, which is a well-established solution in dynamic modeling with low computational cost. The proposed methodology is conducted in the frequency domain and it implicitly adopts the principle of modal superposition, which is applicable to structures of arbitrary geometry and arbitrary dynamic loads. The cantilever beam is the traditional reference problem in many cases of structural analysis thanks to its simple interpretation of natural frequencies and mode shapes. Even if geometry and loads may seem to be limited to "simple" beam-like configuration, the proposed methodology is general.

For the sensitivity analysis, a GSA using the variance-based indices proposed by Sobol in 1993[14] is used. Some interesting features of variance-based methods are model independence, capacity to capture the influence of the full range of variation of the input parameters, and also appreciation of interaction effects among the input parameters.[15]

The main goal of the present work is to propose a framework to study the sensitivity in the input parameters of a model for crack propagation and how they affect the fatigue life predictions and SHM strategies. Recently, Dirlik and Benasciutti[16] pointed out the current small literature available concerning spectral-based methods and crack propagation.[13,17–20] In addition, Datteo et al.[7] indicated the lack of uncertainty assessment in the SHM literature. This paper thus attempts to promote the discussion on both topics and partially fill these gaps by proposing a framework for the sensitivity and uncertainty analysis of beam-like structures concerning crack propagation under spectral loads.

2 | MATHEMATICAL MODEL

The analysis starts with the derivation of the equations of motion of the cantilever beam using the Ritz approach. The mathematical model proposed by Kim and Kim[21] is adopted, who investigated piezoelectric energy harvesters with a distributed tip mass.

2.1 | Equation of motion and frequency response function

Consider a cantilever beam with a distributed tip mass attachment that is subjected to base excitation, as shown in Figure 1.

The beam has thickness t, and the tip mass has a length L_M, a height h_M, a mass M_t, and rotational inertia $J=\frac{1}{12}M_t\left(h_M^2+L_M^2\right)$. The undamped equation of motion for the transverse vibrations of an Euler–Bernoulli cantilever beam under base excitation is given by

$$EI\frac{\partial^4 w_{rel}(x,t)}{\partial x^4}+m_b\frac{\partial^2 w_{rel}(x,t)}{\partial t^2} =-\left[m_b+\overline{M}\delta(x-L_0)-\overline{M}\frac{L_M}{2}\frac{d\delta(x-L_0)}{dx}\right]\frac{\partial^2 w_b(t)}{\partial t^2}, \quad (1)$$

where EI is the bending stiffness of the beam; m_b is the mass of the beam per unit length; $\delta(x)$ is the Dirac delta function; $w_{rel}(x,t)$ is the transverse displacement relative to the clamped end of the beam; $w_b(t)$ is the base displacement; and $\overline{M}$ is the total tip mass at point $x=L_0$, given by

$$\overline{M}=M_t+m_bL_M. \quad (2)$$

Equation (1) is valid in the interval $0\le x\le L_0$. Following the Ritz method, the solution for Equation (1) can be represented as a convergent series:

$$w_{rel}(x,t)=\sum_{r=1}^{\infty}\phi_r(x)\eta_r(t), \quad (3)$$

where $\phi_r(x)$ is the mass normalized eigenfunction and $\eta_r(t)$ is the modal coordinate. Solution of the differential eigenvalue problem and application of the boundary conditions of the cantilever beam with distributed tip mass lead to

$$\phi_r(x)=A_r[(\cosh\lambda_r x-\cos\lambda_r x)-\gamma_r(\sinh\lambda_r x-\sin\lambda_r x)], \quad (4)$$

with γ_r given by

$$\gamma_r=\frac{m_b(\sinh\lambda_rL_0-\sin\lambda_rL_0)+\lambda_r\overline{M}\left(\cos\lambda_rL_0-\cosh\lambda_rL_0+\frac{L_M}{2}\lambda_r(\sinh\lambda_rL_0+\sin\lambda_rL_0)\right)}{m_b(\cosh\lambda_rL_0+cos\lambda_rL_0)+\lambda_r\overline{M}\left(\sinh\lambda_rL_0-\sin\lambda_rL_0+\frac{L_M}{2}\lambda_r(\cosh\lambda_rL_0-\cos\lambda_rL_0)\right)}. \quad (5)$$

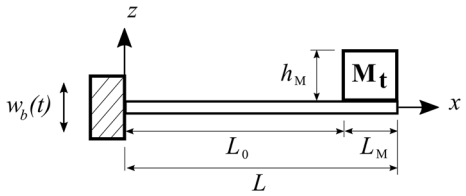

FIGURE 1 Cantilever beam with tip mass attachment under base excitation

The modal amplitude A_r is found by evaluating the normalized eigenfunctions according to one of two orthogonality conditions:

$$\int_0^{L_0}\phi_s(x)m_b\phi_r(x)dx+\phi_s(L_0)\overline{M}\left(\phi_r(L_0)+\frac{L_M}{2}\frac{d\phi_r(L_0)}{dx}\right)+\frac{d\phi_s(L_0)}{dx}\left(J_0\frac{d\phi_r(L_0)}{dx}+\frac{L_M}{2}\overline{M}\phi_r(L_0)\right)=\delta_{rs}, \quad (6)$$

$$\int_0^{L_0} \phi_s''(x) EI \phi_r''(x) dx = \omega_r^2 \delta_{rs}, \tag{7}$$

where δ_{rs} is the Kronecker delta and the double primes denote the second differentiation with respect to x. The inertia term J_0 can be found from

$$J_0 = J + M_t\left(\left(\frac{L_M}{2}\right)^2 + \left(\frac{h_M}{2}+\frac{t}{2}\right)^2\right) + m_b L_M \left(\frac{L_M}{2}\right)^2. \tag{8}$$

The undamped natural frequency, ω_r, can be obtained from

$$\omega_r = (\lambda_r L_0)^2 \sqrt{\frac{EI}{m_b L^4}}. \tag{9}$$

The dimensionless eigenvalues, λ_r, are calculated from the characteristic equation:

$$\begin{aligned} &1 + \cos\lambda_r L_0 \cosh\lambda_r L_0 + \frac{\lambda_r L_0 \overline{M}}{m_b L_0}\Big(\cos\lambda_r L_0 \sinh\lambda_r L_0 \\ &-\sin\lambda_r L_0 \cosh\lambda_r L_0\Big) - \frac{(\lambda_r L_0)^3 J_0}{m_b L_0^3}\Big(\cosh\lambda_r L_0 \sin\lambda_r L_0 \\ &+\sinh\lambda_r L_0 \cos\lambda_r L_0\Big) + \frac{(\lambda_r L_0)^4 J_0 \overline{M}}{(m_b L_0)^2 L_0^2}(1-\cos\lambda_r L_0 \cosh\lambda_r L_0) \\ &- \frac{(\lambda_r L_0)^2 \overline{M} L_M}{m_b L_0^2}\sinh\lambda_r L_0 \sin\lambda_r L_0 \\ &- \frac{(\lambda_r L_0)^4 \overline{M}^2 L_M^2}{4(m_b L_0)^2 L_0^2}(1-\cos\lambda_r L_0 \cosh\lambda_r L_0) \\ &= 0. \end{aligned} \tag{10}$$

From Equation (3) and the boundary conditions, Equation (1) may be re-written as

$$M_{rs}\ddot{\eta}_r(t) + K_{rs}\eta_r(t) = F_r \ddot{w}_b(t), \tag{11}$$

where M_{rs} and K_{rs} are, respectively, the equivalent mass and stiffness matrix, given by

$$\begin{aligned} M_{rs} = \int_0^{L_0} \phi_s(x) m_b \phi_r(x) dx \phi_s(L_0)\overline{M}\left(\phi_r(L_0) + \frac{L_M}{2}\frac{d\phi_r(L_0)}{dx}\right) + \\ \frac{d\phi_s(L_0)}{dx}\left(J_0 \frac{d\phi_r(L_0)}{dx} + \frac{L_M}{2}\overline{M}\phi_r(L_0)\right), \end{aligned} \tag{12}$$

$$K_{rs} = \int_0^{L_0} \phi_s''(x) EI \phi_r''(x) dx, \tag{13}$$

and with forcing function:

$$F_r = -m_b \int_0^L \phi_r(x) dx - \overline{M}\phi_r(L_0) + \overline{M}\frac{L_M}{2}\frac{d\phi_r(L_0)}{dx}. \tag{14}$$

From the orthogonality conditions, the equation of motion (10) reduces to

$$\ddot{\eta}_r(t) + \omega_r^2 \eta_r(t) = F_r \ddot{w}_b(t). \tag{15}$$

To include the effects of damping in a viscous damping model, a modal damping term ζ_r proportional to the velocity $\dot{\eta}_r(t)$ is inserted in Equation (15), leading to

$$\ddot{\eta}_r(t) + 2\zeta_r \omega_r \dot{\eta}_r(t) + \omega_r^2 \eta_r(t) = F_r \ddot{w}_b(t). \tag{16}$$

With harmonic base excitation of the form $w_b(t) = \overline{W}_0 e^{i\omega t}$ (where W_0 is the base displacement amplitude and ω is the excitation frequency), the steady-state modal response is also harmonic of the form $\eta_r(t) = \overline{N}_r e^{j\omega t}$. Equation (16) then yields

$$\overline{N}_r = \frac{\omega^2\left(m_b \int_0^L \phi_r(x) dx + M_t \phi_r(x)\delta(x-L)\right)}{\omega_r^2 - \omega^2 + j2\zeta_r\omega_r\omega}\overline{W}_0. \tag{17}$$

To determine the dynamic stresses on the beam, the bending moment $M(x,t)$ is calculated as the product of beam cross-sectional stiffness and curvature:

$$M(x,t) = EI\frac{\partial^2 w_{rel}(x,t)}{\partial x^2}, \tag{18}$$

and the normal stresses due to bending moment are given by

$$S(x,t) = \frac{M(x,t)h}{I}, \tag{19}$$

where h is the distance from the neutral line of the beam and I the moment of inertia.

We now define a transfer function $H_{Sa}(\omega)$ that relates the normal stress to the base acceleration applied to the beam:

$$H_{Sa}(\omega) = \frac{S}{\ddot{w}_b}. \tag{20}$$

Combining Equations (17), (18), and (19) into Equation (20) yields

$$H_{Sa}(\omega) = -hE\sum_{r=1}^{\infty} \frac{\phi_r''(x)\left[m_b \int_0^L \phi_r(x)dx + M_t\phi_r(x)\delta(x-L)\right]}{\omega_r^2 - \omega^2 + j2\zeta_r\omega_r\omega}, \tag{21}$$

where E is Young's modulus. Notice that although the notation of $H_{Sa}(\omega)$ refers only to its dependency on the excitation frequency, it is also a function of the longitudinal position x, meaning it can be used to obtain the stress transfer function at any point along the length of the beam.

For the case of spectrum loads, the base excitation is better described by its power spectrum density (PSD). Let $G_a(\omega)$ be the one-sided PSD of the applied base acceleration. Then, the PSD of the stress response, $G_{SS}(\omega)$, can be calculated from

$$G_{SS}(\omega) = |H_{Sa}(\omega)|^2 G_a(\omega). \tag{22}$$

In Equation (22), both the excitation and the stress response are random processes, which can only be characterized in a statistical sense. The equation expresses the relation between the stress response of the structure and the excitation spectrum, with the transfer function accounting for the effect of vibrational modes.

2.2 | Fatigue life under random loads

Once the stress PSD is calculated, spectral-based methods can be used to determine the probability density function (PDF) of the stress response. It is worth noticing that the PSD of a stationary Gaussian process can be further divided into narrow-band and wideband processes.[22] In the narrow-band range, the method known as narrow-band solution, proposed by Bendat,[23] is usually employed. The method is built on the fact that, for a narrow-band process, the stress distribution follows the form of a Rayleigh distribution. The PDF of the stress response can then be calculated as

$$p(S_a) = \frac{S_a}{\sigma^2}\exp\left(-\frac{S_a^2}{2\sigma^2}\right), \tag{23}$$

where S_a is the stress amplitude and σ is the standard deviation, which for a process with zero mean can be obtained from the squared root of the zeroth-order spectral moment of the stress process, m_0:

$$m_0 = \int_0^{\infty} G_{xx}(f)df, \tag{24}$$

where f denotes frequency, in Hertz, and $G_{xx}(f)$ is the one-sided PSD of the stress response. The mean upcrossing frequency of the process can be estimated from:

$$\nu_0 = \sqrt{\frac{\int_0^{\infty} f^2 G_{xx}(f)df}{\int_0^{\infty} G_{xx}(f)df}}. \tag{25}$$

For wideband processes, approximate solutions such as the ones proposed by Dirlik[24] or Benasciutti and Tovo[25] could be employed.

In the linear elastic fracture mechanics approach, the rate of crack propagation, da/dN, can be described by the Walker equation as a function of the SIF range as shown in Equation (26):

$$\frac{da}{dN} = \frac{C_0}{(1-R)^{n(1-\gamma)}}(\Delta K)^n, \tag{26}$$

where ΔK is the SIF range; R is the stress ratio; and C_0, n, and γ are material parameters. The SIF range assumes the generic form in linear fracture mechanics:

$$\Delta K = \Delta S.F(a).\sqrt{a}, \tag{27}$$

in which ΔS is the stress range; $F(a)$ is the geometrical factor, which is a function of the component geometry, of the load case in the vicinity of the crack tip, and the crack size, a. The stress range is related to the stress amplitude, S_a, by

$$\Delta S = 2S_a. \tag{28}$$

Two initial simplification hypotheses used in this work are that the stress cycles caused by the spectrum loads are fully reversed (which implies a constant stress

ratio of $R=-1$) and that compressive stresses do not affect the rate of crack propagation (i.e., $\gamma=0$). Due to these assumptions, the crack propagation law assumes the form of the original equation proposed by Paris–Erdogan, in which the only material parameters are C_0 and n. Thus, Equation (26) is simplified into

$$\frac{da}{dN}=C_0\left(S_a.F(a).\sqrt{a}\right)^n. \tag{29}$$

Considering the particular case of crack propagation, an equivalent stress amplitude can be obtained from a random stress process with zero mean according to the equation[13,19]:

$$S_{eqv}=\left[\int_0^\infty S_a^n p(S_a)dS_a\right]^{\frac{1}{n}}. \tag{30}$$

The fatigue life N_t can then be estimated by integration of Equation (29) from an initial crack length, a_i, to a final/critical length a_f:

$$N_t=\int_{a_i}^{a_f}\frac{da}{C_0\left(S_{eqv}F(a)\sqrt{a}\right)^n}. \tag{31}$$

2.3 | Response of cracked beams and damage indices

For the sake of evaluating the coupling between the uncertainties in an SHM system and the prediction of the RUL of a structure, a simple model for the reduction in natural frequency of a beam due to the presence of cracks is investigated.

The dynamic response and natural frequency reduction of cracked beams have been extensively studied in the literature.[26–28] When there is a crack in the structure, the energy E^c consumed for crack growth can be calculated from fracture mechanics according to the following expression[29]:

$$E^c=\int GdA_c, \tag{32}$$

where G is the strain energy release rate (SERR) and A_c is the cracked area. The SERR is calculated as a function of the SIF K_I:

$$G=\frac{K_I^2}{E'}, \tag{33}$$

where $E'=E$ for plane stress and $E'=E/(1-\nu^2)$ for plane strain conditions, with ν the Poisson ratio.

For the geometry used in this work, the damage condition was assumed to be that of edge cracks propagating symmetrically along the cross-section of the beam, as shown in Figure 2. Strip thickness t is much smaller than strip width $2b$. The SIF of a strip with edge cracks propagating symmetrically from both sides and subjected to a constant bending moment is given by Murakami[30]:

$$K_I=F(a)S_x\frac{b}{b-a}\sqrt{b-a}, \tag{34}$$

where b is half the width of the strip, as shown in Figure 2; c is half the distance between the two crack fronts; and S_x is the stress induced by the bending moment M. For the numerical evaluation of Equation (31), the geometry factor $F(a)$ is interpolated from the values given by Murakami,[30] as shown in Figure 3.

Combining Equations (19), (33), and (34) into Equation (32) yields

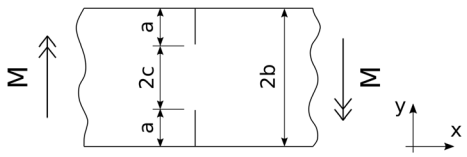

FIGURE 2 Strip with edge cracks subjected to bending moment

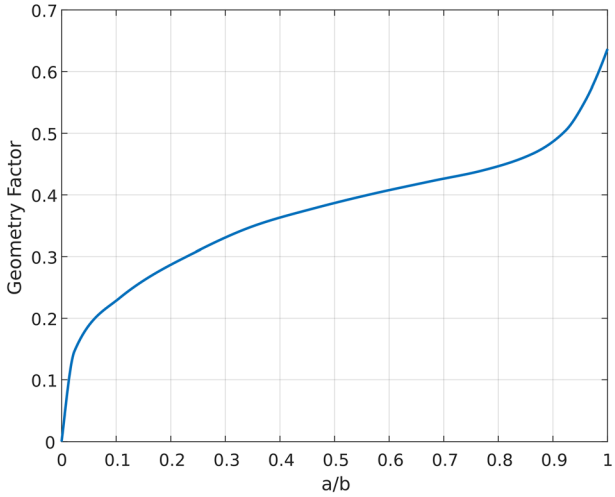

FIGURE 3 Geometry factor used in the model [Colour figure can be viewed at wileyonlinelibrary.com]

$$E^c = \frac{\eta^2(t)}{E'}\left[\left(\frac{Ebt}{2}\right)^2 \phi_r''(x)\phi_s''(x)\delta(x-x_c)\right]\int_0^{a_s} t\frac{F(a)^2}{b-a}da, \tag{35}$$

where x_c is the crack position along the x direction, t is the thickness of the beam, and a_s is the crack size.

As a first approximation of the response of the cracked beams, the mode shapes are assumed unchanged from the pristine condition, when there are no cracks in the structure. According to Afshari and Inman,[31] when using the mode shapes of the un-cracked beam, the maximum strain energy needs to be modified to account for the loss of energy due to the presence of the crack. The equivalent stiffness matrix for the cracked beam is thus written as

$$K_{rs}^c = EI\int_0^L \phi_r''(x)\phi_s''(x)dx - \frac{2}{E'}\left[\left(\frac{Ebt}{2}\right)^2 \phi_r''(x)\phi_s''(x)\delta(x-x_c)\right]\int_0^{a_s} t\frac{F(a)^2}{b-a}da. \tag{36}$$

While the natural frequencies of the cracked beam may be found from the eigenvalue problem:

$$\left(-\omega^2 M_{rs} + K_{rs}^c\right)\overline{N}_r = 0. \tag{37}$$

Damage indices constitute an important aspect of the SHM philosophy. Damage indices based on vibrational response often rely on changes in the structure's modal parameters to return a scalar value that quantifies how much the structure has changed. The most useful damage-finding methods in this scenario are the ones that use changes in resonance frequency since they are reliable and easy to obtain.[32]

A damage index (DI) is introduced to investigate the evolution of the damage due to crack growth. The proposed DI is based solely on natural frequency shifts, according to the formula:

$$DI = \sum_1^j \frac{\left|\omega_j^i - \omega_j^d\right|}{\omega_j^i} \times 100, \tag{38}$$

where ω_j is the natural frequency of the jth vibrational mode and the superscripts i and d denote, respectively, the pristine and damaged condition of the structure. In the present work, DI is assumed to be the sum of the percentual change in natural frequencies.

3 | RANDOMIZED INPUTS

A sensitivity analysis is used to determine which parameter influences the most in the variation of the model. For the UQ, the input parameters of the model adopt values that are represented by their PDFs, and then, a conclusion can be made regarding the model's output average, standard deviation, distribution, and so on. Both analyses are carried out by the Matlab-based software UQLab.[33,34]

For the sake of illustrating the proposed framework, the same geometry employed by the authors previously is used.[13] The cantilever beam is made from an aluminum sheet in Al7075-T6, with 1.27 mm thickness, with the other dimensions as shown in Figure 4. The free length of the beam has a total mass of 11 g, and a small tip mass of 4.5 g (dimensions of $L_M = 10$ mm and $h_M = 5$ mm, as per Figure 1) is glued to the tip of the beam. To evaluate the crack propagation phenomenon, the beam has premachined edge cracks distant 25 mm away from the clamping region.

For the experimental modal analysis, an intact beam (without edge cracks) is clamped into a grip that is considered to be theoretically rigid and it is then mounted on an electrodynamic shaker, subjecting the specimen to a base excitation condition. The structural stress response is recorded using a resistive strain gage fixed at point SG shown in Figure 4, while an accelerometer is fixed at the clamp to measure the input base acceleration applied in the z-direction.

The material constants and geometry are considered as the uncertain parameters. To quantify the uncertainty in the fatigue life of the structure, the crack propagation law is also randomized. Different stochastic crack

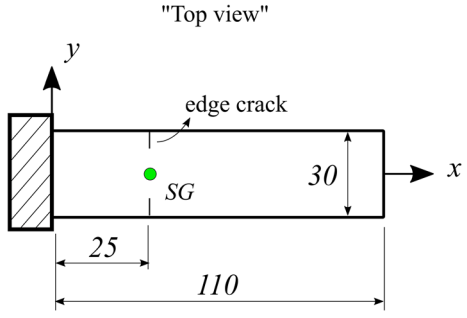

FIGURE 4 Geometry of the cantilever beam (not to scale)—units in mm [Colour figure can be viewed at wileyonlinelibrary.com]

propagation models are available in the literature, such as the models based on the Markov chain,[35,36] on polynomial chaos,[37] or on a jump process.[38,39] Another possibility is to use random differential equation models in which, according to Maymon,[40] two major approaches can be devised: The use of a modified differential equation for crack growth where the stochastic nature is expressed by a random process; or the use of a deterministic equation while assuming that its model parameters are random variables. The latter option is used in this work.

Due to the previous assumptions, the crack propagation law assumes the form of the original equation proposed by Paris–Erdogan, and the only material parameters are C_0 and n. It has long been (empirically) observed that these two parameters are correlated.[41–43] Due to this observation, some authors have proposed that these two parameters should not be assumed simultaneously as random independent variables.[44] Sanches et al.[44] then proposed that the scatter in fatigue life could be represented by fixing the exponent n to its experimental average value and modeling C_0 according to a lognormal distribution. The same approach is used here.

The mean value of C_0 and the fixed value for n are taken from Dowling[45] ($C_0 = 2.71 \times 10^{-8} \left(\frac{\text{mm/cycle}}{(\text{MPa}\sqrt{\text{m}})^n}\right)$ and $n = 3.70$), while the variance in C_0 is set in order to accommodate the scatter observed in the experimental results of Hudson and Scardina,[46] who analyzed the fatigue crack propagation in 46 specimens of a 7075-T6 aluminum alloy at stress ratios ranging from $R = -1.0$ to 0.8. The data obtained by Hudson and Scardina are plotted according to the Walker equation, with $\gamma = 0$ for negative stress ratios and $\gamma = 0.641$ for positive values of R.[45] C_0 is thus modeled as a lognormal distribution with a standard deviation of $6.32 \times 10^{-9} \left(\frac{\text{mm/cycle}}{(\text{MPa}\sqrt{\text{m}})^n}\right)$.

Figure 5 shows the experimental data collected by Hudson and Scardina, along with 15 randomly generated crack propagation curves from variations of C_0.

To obtain the fatigue life, Equation (31) is integrated from an initial crack size until the critical size. The critical crack size depends on the fracture toughness of the material and on the maximum applied load, which in this case is random. The literature reports a fracture toughness in the range of 24.2 to 30.3 $\text{MPa}\sqrt{\text{m}}$ for the TL orientation of the plate,[47] so this value will be taken as reference, assuming that it follows a normal distribution around the mean value with an interval of six times the standard deviation. For the maximum applied load, the $\pm 3\sigma$ criterion is used,[17] which assumes that the maximum stress is equal to three times the standard deviation

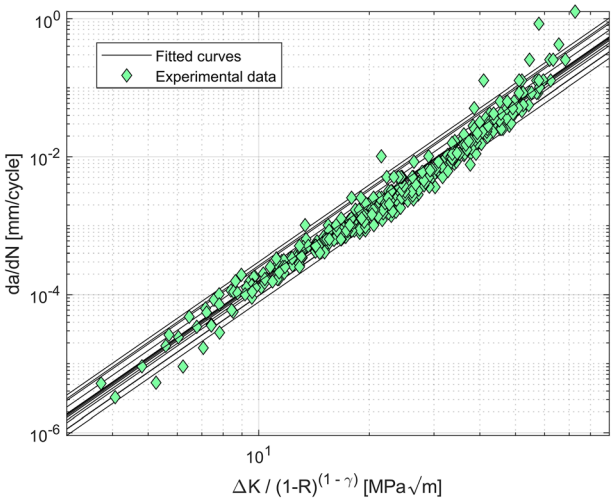

FIGURE 5 Experimental data points and simulated fitting equations for crack propagation in 7075-T6 aluminum alloy [Colour figure can be viewed at wileyonlinelibrary.com]

of the stress process, which for a given Gaussian random distribution is actually a deterministic number.

The specimens tested are machined by a wire-cut electrical discharge machining (WEDM). The dimensional accuracy of the WEDM process was experimentally examined by Islam et al.,[48] who calculated a surprisingly high international tolerance (IT) grade of almost 12 in the linear dimensional error of the process. Thus, an IT 12 will be used as reference to estimate the standard deviation of the geometrical dimensions of the specimens used in this work. The geometric dimensions are then assumed to follow a normal distribution around its nominal value with a tolerance (as given by the ISO IT12) equivalent to six times the standard deviation. For the elastic properties of the beam (Young's modulus and Poisson ratio), a standard deviation of 0.5% from the nominal properties is used. This value is based on the variation reported by Benedetti et al.,[49] who studied the variability in mechanical properties of extruded aeronautical grade aluminum alloy 7075-T6. The density of the beam and the value of the added tip mass are assumed to follow a Gaussian distribution with 1% standard deviation.

Damping is particularly difficult to model in a structure and, as pointed out by Adhikari,[50] it depends on physical dissipation mechanisms that are not always totally understood. For damping, even the model is not certain, so the damping parameters should exhibit scatter to generate sensible results. In this work, damping is modeled following the standard procedure of modal damping ratio, an approach commonly used in modal analysis. Three experimental measures of the modal damping associated with the first vibrational mode of the

beam with tip mass revealed the values of 0.27%, 0.30%, and 0.33%.[13] As such, damping is modeled with a uniform distribution ranging from 0.25% to 0.35%.

Finally, the stress ranges will also have an important influence on the fatigue life, as they may be seen as the driving force opening the crack. For the case studied in this work, the stress ranges are naturally random, but strongly related to the shape (envelope) and amplitude of the input base acceleration PSD, as shown by Equation (23). Concerning its shape, the input PSD is regarded as being constant in a frequency range of 34 to 100 Hz, but its amplitude is assumed to follow a uniform distribution, varying from 0.17 to 0.23 g^2/Hz. All input parameters used in the sensitivity analysis are shown in Table 1.

4 | FINITE ELEMENT MODEL

The intact beam is modeled in finite elements using Abaqus™. The beam, including its tip mass, is modeled with 47,600 second-order solid elements and reduced integration (C3D20R). The beam has a free length of 110 mm, as displayed in Figure 4. A frequency step is created, followed by a steady-state dynamics modal analysis, which is used to obtain the stress FRF due to base acceleration at point SG, also shown in Figure 4. For the modal analysis, the experimental values of the damping ratios are used.

A finite element model is also built for a cracked beam for the sake of comparing the reductions in natural frequencies caused by the presence of a symmetrical edge crack with the values predicted by the model discussed in Section 2.3. The cracked beam is modeled with approximately 60,000 C3D20R elements, which were proven sufficient by a convergence analysis. The symmetric edge crack is modeled using the "crack" feature available in Abaqus™ by assigning the appropriate crack front and "seam" length. Figure 6 shows the geometry and details of the mesh used to model an 8 mm long edge crack.

5 | MODEL VALIDATION

The first step before considering the sensitivity and UQ analysis is to validate the mathematical description of the structure. An experimental modal analysis of an intact beam (i.e., with no edge cracks) is conducted using an LMS. Scadas equipment linked to Test Lab software. An electromechanical shaker then applies a chirp signal

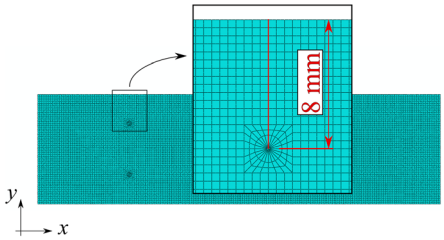

FIGURE 6 Geometry and detail of the mesh around the crack used in the numerical analysis [Colour figure can be viewed at wileyonlinelibrary.com]

TABLE 1 Probability distribution of the input parameters

Parameter	Distribution type	Mean value	Standard deviation
Young's modulus (MPa)	Gaussian	71,016	355
Poisson (-)	Gaussian	0.33	1.65e-3
Density (kg/m^3)	Gaussian	2796	27.96
Length (mm)	Gaussian	110	5.8e-2
Width (mm)	Gaussian	30	3.5e-2
Thickness (mm)	Gaussian	1.27	1.67e-2
Tip mass (kg)	Gaussian	4.5e-3	4.5e-5
Tip mass length (mm)	Gaussian	10	2.5e-2
Tip mass height (mm)	Gaussian	5	2e-2
Crack position (mm)	Gaussian	25	3.5e-2
Fracture toughness (MPa$\sqrt{\text{m}}$)	Gaussian	27.25	1.02
Modal damping (-)	Uniform	0.25% to 0.35%	-
PSD amplitude (g^2/Hz)	Uniform	0.17 to 0.23	-
$C_0 \left(\frac{\text{mm/cycle}}{(\text{MPa}\sqrt{\text{m}})^n}\right)$	Lognormal	2.71e-8	6.32e-9

from 10 up to 2048 Hz with a frequency resolution of 0.125 Hz, and the stress response is registered by a resistive strain gage, which measures the stress at point SG shown in Figure 4. Table 2 shows the experimental natural frequencies and damping ratios of the first three bending modes of the structure.

Figure 7 shows the excellent agreement between the method and the experimentally obtained FRF of the stress response due to base acceleration for point SG. Figure 7 also includes the numerical results obtained from the finite element method (FEM). The experimental values of the damping ratios are used in both numerical models.

To validate the natural frequency reduction obtained from the Ritz method combined with the fracture mechanics approach, the results for three different crack sizes are compared with the ones obtained from the finite element model. The natural frequencies of the first three bending modes of the cracked cantilever beam are shown in Table 3, and the relative difference of the Ritz method is calculated using as reference the results from the finite element model.

The procedure for fatigue life estimation under random loads using the PDF of the stress amplitudes is investigated by the authors in Marques et al.,[13] where an experimental study was conducted for a symmetrical edge crack propagating from an initial size of 7 mm until complete failure of the specimen. Table 4 shows both the experimental result and the predicted fatigue life from the Ritz method and narrow-band solution (using all parameters and properties with nominal values).

6 | RESULTS

As mentioned previously, the main goal of this paper is to propose a framework for the sensitivity and uncertainty analyses considering crack propagation in beams subjected to random loads. In a real-world application of SHM systems, one may be interested in obtaining the probabilistic RUL of the structure. In general, as well known and shown by Aeronautical Structure Group (GEA) from University of Sao Paulo, an SHM system relies on a network of sensors and on a non-destructive technique (NDT) such as Lamb waves or vibration-based methods[51–54] to evaluate the presence of damage in the structure. The data collected by the sensors can then be extracted and combined in the form of a damage metric in order to build a mapping function between the data and the damage state of the structure ("DI correlation" shown in Figure 8). The mapping function can then later be used to estimate the damage condition (or the "probabilistic crack size") based on measures of the DI collected. A schematic representation of this process is shown in Figure 8.

The framework presented herein mainly concerns the third block shown in Figure 8, which corresponds to the sensitivity and UQ. As it can be seen, a necessary input information for this analysis, alongside the input parameters that were discussed in Section 3, is the crack size that is currently presented in the structure, since it will be used as the initial crack size in the integration of Paris law. The method of detection of the crack will of course depend on the type of SHM system the user has available, which drives important aspects such as the minimum crack size detectable and the confidence in which a certain crack size can be estimated (probabilistic crack size).

6.1 | Damage indices

The uncertainty in the proposed DI (Section 2.3) is evaluated for different crack lengths. The randomized inputs

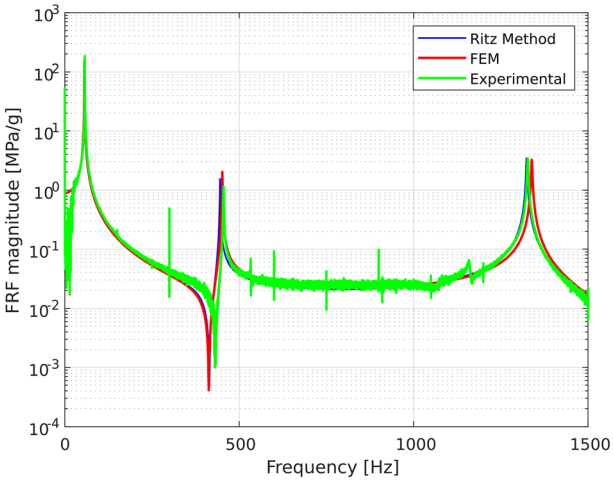

FIGURE 7 Comparison between the Ritz method, the FEM solution, and the experimental value of the stress FRF due to base acceleration. Correlation is very good between both numerical models and the experimental values, and curves are almost coincidental. [Colour figure can be viewed at wileyonlinelibrary.com]

TABLE 2 Experimental natural frequencies and damping ratios of the first three bending modes of the cantilever beam

	1st mode	2nd mode	3rd mode
Natural frequency (Hz)	57.38	455.13	1327.25
Damping ratio	0.30%	0.12%	0.10%

TABLE 3 Natural bending frequencies of the cracked cantilever beam

	1st mode (Hz)	2nd mode (Hz)	3rd mode (Hz)	Crack size
FEM	55.6	451.0	1328.8	$a = 4$ mm
Ritz method	55.1	445.0	1319.7	
Relative difference	−0.9%	−1.3%	−0.7%	
FEM	53.1	448.6	1299.9	$a = 8$ mm
Ritz method	53.8	445.0	1306.5	
Relative difference	1.3%	−0.8%	0.5%	
FEM	48.1	443.9	1245.0	$a = 12$ mm
Ritz method	49.4	444.8	1265.2	
Relative difference	2.7%	0.2%	1.6%	

TABLE 4 Numerical prediction of fatigue life using Ritz model and experimental values[13]

		Fatigue life	
Initial crack	**Number of samples**	**Numerical prediction**	**Experimental (mean)**
7 mm	5	53.3 min	61.8 min

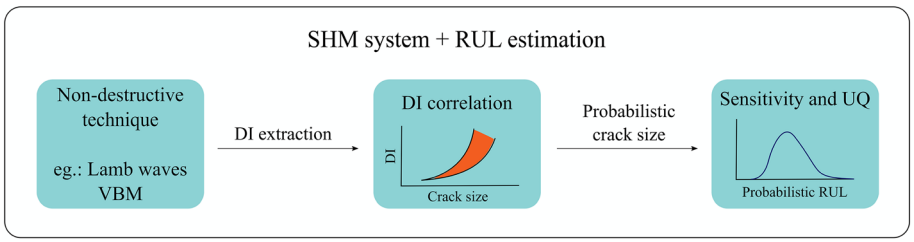

FIGURE 8 Schematic representation of a process combining SHM and sensitivity and uncertainty analyses [Colour figure can be viewed at wileyonlinelibrary.com]

are considered according to the distributions shown in Table 1. Figure 9 shows the DI distributions that are expected at different crack sizes.

The DI based on frequency shifts given in this work is a simple example in a broader context of feature extraction from SHM systems and its correspondence with a certain damage state. It should be noted that SHM measurements are affected not only by uncertainties in material and geometric characteristics but also from imperfect boundary conditions, sensor placement, variations in damage geometry, temperature, electrical and mechanical noise, and so on, which can be addressed, for instance, by means of an online updating Gaussian process, as demonstrated by Chen et al.[10]

In practice, an SHM system obtains a DI through any kind of non-destructive online technique it has implemented and correlates it to the damage state by a previously constructed mapping function, using for instance the results from Figure 9. Due to the uncertainties involved, a DI reading corresponds to a distribution of possible damage states.

To emulate a real-world application of the proposed framework, the DI model developed in Section 2.3 ("Direct Model") will be used to simulate the detection of a crack size (the "Probabilistic crack size" input shown in Figure 8). Thus, a Bayesian inversion framework is applied to the DI (forward) model. In the Bayesian inverse problem, a set of measured DI values can be used to update the prior (unknown) distributions of the input model parameters.[55] This procedure is illustrated in Figure 10.

When the structure has a crack size of 8 mm, the uncertainty analysis showed that the DI follows a lognormal distribution with a mean of 4.40 and a variance of 3e-3 (Figure 9). To simulate some possible readings of an SHM system when the crack is at this stage, a set of 10 DI values are randomly generated according to the obtained distribution, and these values are used as input for the inverse problem. The prior distributions of material properties and geometries are kept the same as shown in Table 1. The prior crack size distribution is then set as a Gaussian distribution with a mean of 10 mm and a standard deviation of 1 mm.

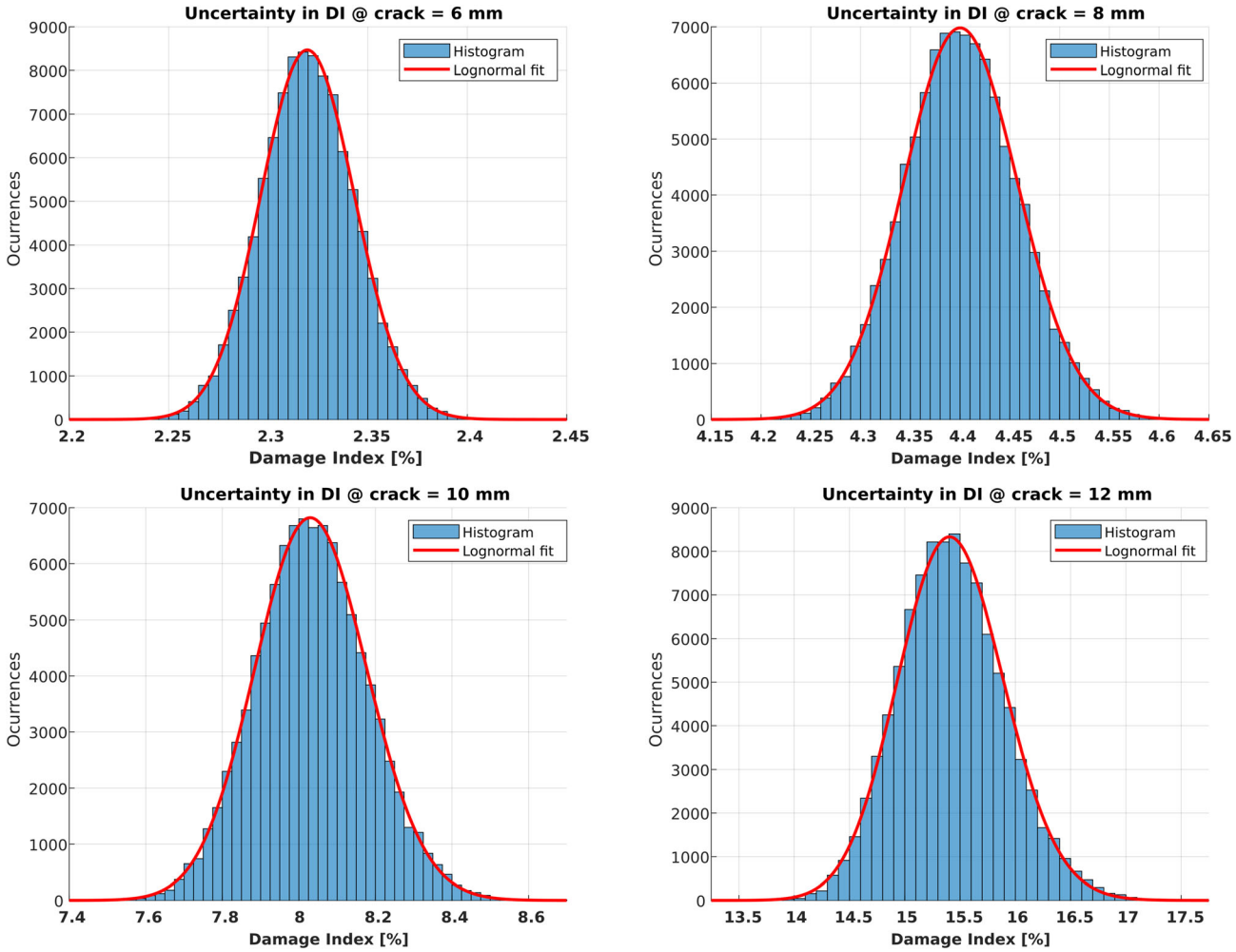

FIGURE 9 Uncertainty in damage index values at different crack sizes [Colour figure can be viewed at wileyonlinelibrary.com]

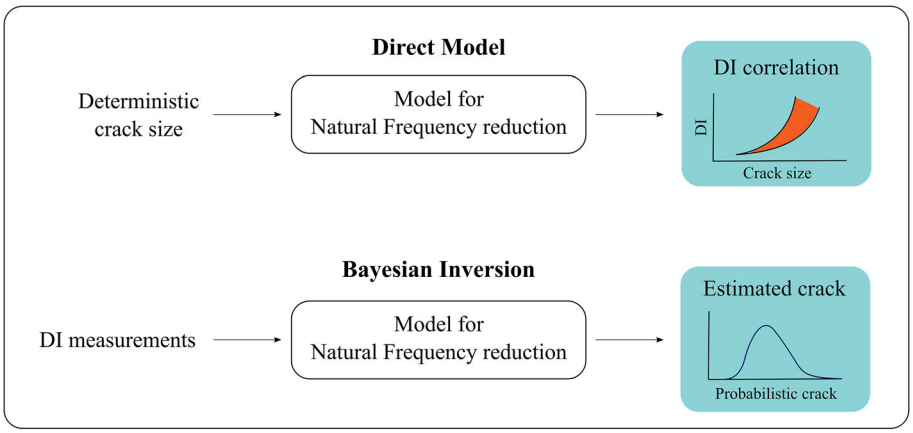

FIGURE 10 Schematic procedure used to obtain a probabilistic crack size [Colour figure can be viewed at wileyonlinelibrary.com]

The Bayesian inversion is carried out in UQLab software.[33,56] The Markov chain Monte Carlo method is used to sample the posterior distributions of the unknown parameters, and 3×10^4 sample points are used. The software then returns an updated distribution for the crack size as a Gaussian distribution with a mean of 8.1 mm mean and standard deviation of 0.21 mm, which is subsequently used as input for the sensitivity and uncertainty analysis in the fatigue life estimation.

6.2 | Sensitivity and uncertainty in fatigue life

The sensitivity analysis of the fatigue life of the structure is conducted in UQLab software[33,34] using its sensitivity tool and Sobol's method. The computational cost of the method is given by $(M_i + 2) \times N$, where M_i is the number of inputs and N is the sample size. The total number of inputs used in the formulation of the problem is 15, and a sample size of 10^5 is used, resulting in $1,700,000$ evaluations of the computational model. Furthermore, the Latin hypercube sampling scheme was adopted.

Figure 11 summarizes the results of the sensitivity analysis. Sobol's indices of order 1 represent the contribution of each input parameter to the variance of the output. The total indices, on the other hand, quantify the interaction effects between model inputs. A total index that equals zero or is approximately zero indicates that the respective input parameter does not contribute to scattering on the RUL.[15]

It can be seen that the Walker parameter C_0 is the most significant parameter contributing to the scatter in the analysis. This is to be expected, given the role played by the parameter in modeling the rate of crack propagation. The results show a large variation in the calculated fatigue life, which may be attributed, in part, to the expected natural variation of the crack propagation phenomena, since the variation in C_0 was set to correspond best to the experimental scatter observed in the crack propagation tests.

The second most important parameter influencing the fatigue life is the modal damping ratio, followed closely by the PSD amplitude. Again, this is no surprise as damping always affects response amplitudes directly in the vicinity of resonance. The modal damping influences the peak amplitude of the FRF of the stress response in the structure, and thus has a direct effect on the amplitude of the PSD of the stress response, affecting the stress PDF given by the narrow-band solution. Likewise, the amplitude of base excitation (PSD amplitude parameter) affects the stress response in a similar manner.

These results also reveal the importance of correctly asserting the damping values in the mathematical model used to describe the structure's dynamic response. Since damping values are usually obtained from an experimental modal analysis, this highlights the importance of a proper experimental assessment of the structure.

The initial crack size parameter was shown to have only a moderate impact on the variance of the results. However, its influence is expected to be higher at small crack sizes, given that crack growth rates are smaller in this condition, so even minor variations in this parameter may bring a large variation in the results.

The probabilistic distribution observed in the fatigue life, shown in Figure 12, was fitted by a lognormal distribution, revealing a mean value of 1.13e+05 cycles and a

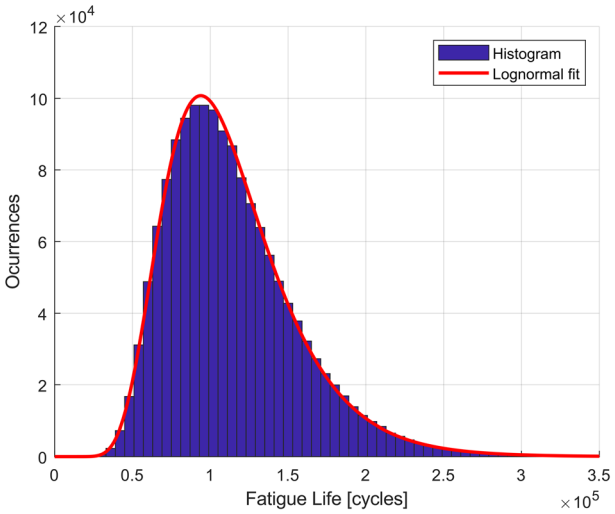

FIGURE 12 Expected distribution of the structure's fatigue life according to the variation of the input parameters given in Table 1 [Colour figure can be viewed at wileyonlinelibrary.com]

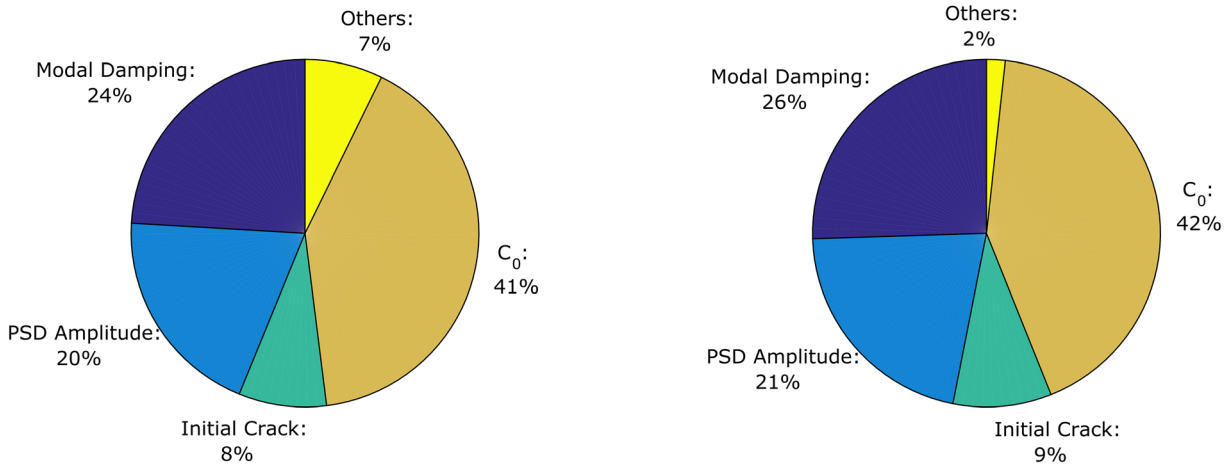

FIGURE 11 Sobol's indices of order 1 (left) and total order (right) for the RUL [Colour figure can be viewed at wileyonlinelibrary.com]

standard deviation of 4.18e+04 cycles. It should be noted that although a somewhat large variance was assumed for the geometric and material properties (Young's modulus and Poisson) of the structure, the large scatter observed in the fatigue life of the structure is mostly due to the variance of coefficient C_0 from Walker's equation, as shown by the results of the GSA. The values of modal damping and the amplitude of the PSD excitation also have a non-negligible impact in the structure's life.

As pointed out by Leser et al.,[12] SHM systems usually provide information about the current damage state, while a more comprehensive approach would also involve the propagation of this information to predict the RUL of the structure. Following the proposed approach, the information collected from an SHM system on the current damage state of a structure can be used in a probabilistic assessment of its RUL. At the same time, SHM systems that do not consider the inherent variability in materials and mechanical process may suffer with erroneous identification of damage in their structures.

7 | CONCLUSIONS

A framework is presented for the sensitivity and uncertainty analysis of fatigue crack growth under random loads. A study case is investigated for a structure that uses shifts in the natural frequencies as a DI and correlates it to the crack size, but that can be easily generalized to different SHM approaches. The methodology enables the study of the probabilistic RUL of beam-like structures under random loads with low computational cost. The potential of the methodology also lies in the fact that the vibration of many structures can be analyzed by modeling it in the simplest way as a beam.[57] With the present case study, the results show that the coefficient C_0 from Walker's equation has the most impact on the fatigue life of the component. The modal damping factor and the amplitude of the input acceleration were also identified as important parameters affecting the variance of the results. The framework presented can be used in complement to SHM systems to allow a deeper understanding of the influence of each parameter and their uncertainties in the response of the structure, while also helping in its reliability analysis. If not properly addressed, these natural variations in material properties and geometry can make SHM systems impracticable or even cause the premature failure of the structure.

ACKNOWLEDGMENTS

This study was financed in part by the Coordenação de Aperfeiçoamento de Pessoal de Nível Superior—Brasil (CAPES) (Finance Code 001). Volnei Tita acknowledges the financial support of the National Council for Scientific and Technological Development (CNPq process number: 310656/2018-4).

CONFLICT OF INTEREST

The authors declare that they have no conflicts of interest.

AUTHOR CONTRIBUTIONS

Denys Marques: Conceptualization; methodology; formal analysis; writing - original draft preparation. **Dirk Vandepitte**: Supervision; writing - review & editing. **Volnei Tita**: Conceptualization; methodology; supervision; writing - review & editing.

DATA AVAILABILITY STATEMENT

The data presented in this manuscript can be made available upon reasonable request.

NOMENCLATURE

a	crack size
a_0	initial crack size
a_f	final crack size
a_c	critical crack size
A_c	cracked area
A_r	modal amplitude
b	half the width of the strip
c	half the distance between two crack fronts on a strip
C_0	material parameter for the Walker equation
da/dN	rate of crack growth per cycle
DI	damage index
E	Young's modulus
E^c	energy consumed for crack growth
EI	beam bending stiffness
f	frequency
$F(a)$	geometrical factor
F_r	forcing function
G	strain energy release rate
$G_{xx}(f)$	one-sided power spectral density
$G_a(\omega)$	base acceleration PSD
$G_{SS}(\omega)$	stress response PSD
h_M	tip mass height
$H_{Sa}(\omega)$	transfer function of stress over base acceleration
J	tip mass rotational inertia
J_0	inertia term
K_I	stress intensity factor for mode I
K_{rs}	stiffness matrix
K^c_{rs}	equivalent stiffness matrix
L	beam length
L_M	tip mass length
m_b	beam mass per unit length

M	bending moment
M_t	tip mass
$\overline{M}$	total tip mass
M_{rs}	mass matrix
m_i	ith-order spectral moment
N_T	number of cycles in a load history
n	exponential parameter for the Walker equation
$p(S)$	probability density function of the stress response
PDF	probability density function
PSD	power spectral density
R	stress ratio
RUL	remaining useful life
S_a	stress amplitude
$S(x,t)$	normal stress due to bending moment
S_f	stress upper limit of truncation
SIF	stress intensity factor
SHM	structural health monitoring
t	beam thickness
$w_b(t)$	base displacement
$w_{rel}(x,t)$	transverse displacement relative to the clamped end of the beam
x_c	crack position
α_i	ith-order spectral width
γ	material parameter of the Walker equation
γ_r	parameter of the normalized eigenfunction
δ_{rs}	Kronecker delta
$\delta(x)$	Dirac delta function
ΔK	stress intensity factor range
ΔS	stress range
λ_r	dimensionless eigenvalue
$\eta_r(t)$	modal coordinate
$\phi_r(x)$	mass normalized eigenfunction
v	Poisson ratio
ω	excitation frequency
ω_r	undamped natural frequency
ζ_r	modal damping

ORCID

Denys Marques https://orcid.org/0000-0001-5864-0017

REFERENCES

1. Tavares SMO, Castro MST. An overview of fatigue in aircraft structures. *Fatigue Fract Eng Mater Struct*. 2017;40(10):1510-1529.
2. Ren H, Chen X, Chen Y. Chapter 9—Structural health monitoring and influence on current maintenance. In: *Reliability Based Aircraft Maintenance Optimization and Applications*. Academic Press; 2017:173-184.
3. Sartorato M, Medeiros R, Vandepitte D, Tita V. Computational model for supporting SHM systems design: damage identification via numerical analyses. *Mech Syst Signal Pr*. 2017;84:445-461.
4. Tcherniak D, Mølgaard LL. Active vibration-based structural health monitoring system for wind turbine blade: demonstration on an operating Vestas V27 wind turbine. *Struct Health Monit*. 2017;16(5):536-550.
5. Khodabandehlou H, Pekcan G, Fadali MS. Vibration-based structural condition assessment using convolution neural networks. *Struct Control Health Monit*. 2019;26(2):e2308.
6. de Medeiros R, Vandepitte D, Tita V. Structural health monitoring for impact damaged composite: a new methodology based on a combination of techniques. *Struct Health Monit*. 2018;17(2):185-200.
7. Datteo A, Busca G, Quattromani G, Cigada A. On the use of AR models for SHM: a global sensitivity and uncertainty analysis framework. *Reliab Eng Syst Safe*. 2018;170:99-115.
8. Marques F, Correia JAFO, De Jesus AMP, Cunha A, Caetano E, Fernandes AA. Fatigue analysis of a railway bridge based on fracture mechanics and local modelling of riveted connections. *Eng Fail Anal*. 2018;94:121-144.
9. Kala Z. Global sensitivity analysis of reliability of structural bridge system. *Eng Struct*. 2019;194:36-45.
10. Chen J, Yuan S, Wang H. On-line updating Gaussian process measurement model for crack prognosis using the particle filter. *Mech Syst Signal Pr*. 2020;140:106646.
11. Sankararaman S, Ling Y, Mahadevan S. Uncertainty quantification and model validation of fatigue crack growth prediction. *Eng Fract Mech*. 2011;78(7):1487-1504.
12. Leser PE, Hochhalter JH, Warner JE, et al. Probabilistic fatigue damage prognosis using surrogate models trained via three-dimensional finite element analysis. *Struct Health Monit*. 2017;16(3):291-308.
13. Marques DET, Vandepitte D, Tita V. Damage detection and fatigue life estimation under random loads: a new structural health monitoring methodology in the frequency domain. *Fatigue Fract Eng Mater Struct*. 2021;44(6):1622-1636.
14. Sobol IM. Sensitivity estimates for nonlinear mathematical models. *Math Model Comput Exp*. 1993;1:407-414.
15. Saltelli A, Ratto M, Andres T, et al. *Global Sensitivity Analysis—The Primer*. John Wiley & Sons; 2008.
16. Dirlik T, Benasciutti D. Dirlik and Tovo-Benasciutti spectral methods in vibration fatigue: a review with a historical perspective. *Metals*. 2021;11(9):1333.
17. Zuccarello B, Adragna NF. A novel frequency domain method for predicting fatigue crack growth under wide band random loading. *Int J Fatigue*. 2007;29(6):1065-1079.
18. Mao W. Development of a spectral method and a statistical wave model for crack propagation prediction in ship structures. *J Ship Res*. 2014;58(02):106-116.
19. Xue X, Chen N. Fracture mechanics analysis for a mooring system subjected to Gaussian load processes. *Eng Struct*. 2018;162:188-197.
20. Zhang Y, Huang X, Wang F. Fatigue crack propagation prediction for marine structures based on a spectral method. *Ocean Eng*. 2018;163:706-717.
21. Kim JE, Kim YY. Analysis of piezoelectric energy harvesters of a moderate aspect ratio with a distributed tip mass. *J Vib Acoust*. 2011;133(4):041010.
22. Mrsnik M, Slavic J, Boltezar M. Vibration fatigue using modal decomposition. *Mech Syst Signal Pr*. 2018;98:548-556.

23. Bendat JS. *Principles and Applications of Random Noise Theory*. John Wiley & Sons; 1958.
24. Dirlik T. *Application of Computers in Fatigue Analysis*. Ph.D. Thesis. University of Warwick; 1985.
25. Benasciutti D, Tovo R. Spectral methods for lifetime prediction under wide-band stationary random processes. *Int J Fatigue*. 2005;27(8):867-877.
26. Fernández-Sáez J, Rubio L, Navarro C. Approximate calculation of the fundamental frequency for bending vibrations of cracked beams. *J Sound Vib*. 1999;225(2):345-352.
27. Zhong S, Oyadiji SO. Analytical predictions of natural frequencies of cracked simply supported beams with a stationary roving mass. *J Sound Vib*. 2008;311(1–2):328-352.
28. Zheng T, Ji T. An approximate method for determining the static deflection and natural frequency of a cracked beam. *J Sound Vib*. 2012;331(11):2654-2670.
29. Yang XF, Swamidas ASJ, Seshadri R. Crack identification in vibrating beams using the energy method. *J Sound Vib*. 2001; 244(2):339-357.
30. Murakami Y. *Stress Intensity Factors Handbook*. Pergamon Press; 1987.
31. Afshari M, Inman DJ. Continuous crack modeling in piezoelectrically driven vibrations of an Euler-Bernoulli beam. *J Vib Control*. 2012;19(3):341-355.
32. Gomes GF, Mendez YAD, Alexandrino PSL, Cunha SS Jr, Ancelotti AC Jr. A review of vibration based inverse methods for damage detection and identification in mechanical structures using optimization algorithms and ANN. *Arch Comput Method E*. 2019;26(4):883-897.
33. Marelli S, Sudret B. UQLab: a framework for uncertainty quantification in MATLAB. In: *The 2nd International Conference on Vulnerability and Risk Analysis and Management (ICVRAM 2014)*. University of Liverpool; 2014:2554-2563.
34. Marelli S, Lamas C, Konakli K, Mylonas C, Wiederkehr P, Sudret B. *UQLab User Manual—Sensitivity analysis, Report # UQLab-V1.4-106, Chair of Risk, Safety and Uncertainty Quantification*. ETH Zurich; 2021.
35. Hua Z. An improved probabilistic model of fatigue crack growth. *Eng Fract Mech*. 1993;46(5):773-780.
36. Wu WF, Ni CC. Probabilistic models of fatigue crack propagation and their experimental verification. *Probabilist Eng Mech*. 2004;19(3):247-257.
37. Beck AT, Gomes WJS. Stochastic fracture mechanics using polynomial chaos. *Probabilist Eng Mech*. 2013;34:26-39.
38. Sobczyk K, Trebicki J. Modelling of random fatigue by cumulative jump processes. *Eng Fract Mech*. 1989;34(2): 477-493.
39. Sobczyk K, Trebicki J. Modelling of curvilinear random fatigue crack growth. *Eng Fract Mech*. 1995;52(4):703-715.
40. Maymon G. *Structural Dynamics and Probabilistic Analyses for Engineers*. Butterworth-Heinemann, Elsevier; 2008.
41. Tanaka K, Masuda C, Nishijima S. The generalized relationship between the parameters *C* and *m* of Paris' law for fatigue crack growth. *Scripta Metall*. 1981;15(3):259-264.
42. Cortie MB, Garret GG. On the correlation between the C and m in the Paris equation for fatigue crack propagation. *Eng Fract Mech*. 1988;30(1):49-58.
43. Cortie MB. The irrepressible relationship between the Paris law parameters. *Eng Fract Mech*. 1991;40(3):681-682.
44. Sanches RF, de Jesus AMP, Correia JAFO, da Silva ALL, Fernandes AA. A probabilistic fatigue approach for riveted joints using Monte Carlo simulation. *J Constr Steel Res*. 2015; 110:149-162.
45. Dowling NE. *Mechanical Behavior of Materials—Engineering Methods for Deformation, Fracture, and Fatigue*. 4thed. Pearson; 2013.
46. Hudson CM, Scardina JT. Effect of stress ratio on fatigue-crack growth in 7075-T6 aluminum-alloy sheet. *Eng Fract Mech*. 1969;1(3):429-446.
47. Lai MO, Ferguson WG. Fracture toughness of aluminium alloy 7075-T6 in the as-cast condition. *Mater Sci Eng*. 1985;74(2): 133-138.
48. Islam MN, Rafai NH, Subramanian SS. Dimensional accuracy achievable in wire-cut electrical discharge machining. In: *Electrical Engineering and Applied Computing*. Springer; 2011: 543-553.
49. Benedetti M, Menapace C, Fontanari V, Santus C. On the variability in static and cyclic mechanical properties of extruded 7075-T6 aluminum alloy. *Fatigue Fract Eng Mater Struct*. 2021; 44(11):2975-2989.
50. Adhikari S. *Damping Models for Structural Vibration*. Ph.D. Thesis. Cambridge University; 2000.
51. de Medeiros R, Borges EN, Tita V. Experimental analyses of metal-composite bonded-joints: damage identification. *Applied Adhesion Sci*. 2014;2(1):1-7.
52. de Medeiros R, Sartorato M, Vandepitte D, Tita V. A comparative assessment of different frequency based damage detection in unidirectional composite plates using MFC sensor. *J Sound Vib*. 2016;383:171-190.
53. Medeiros R, Souza GS, Marques DET, Flor F, Tita V. Vibration-based structural health monitoring of bi-clamped metal-composite bonded joint: experimental and numerical analyses. *J Adhesion*. 2021;97(10):891-917.
54. de Menezes VG, Souza GS, Vandepitte D, Tita V, de Medeiros R. Defect and damage detection in filament wound carbon composite cylinders: a new numerical-experimental methodology based on vibrational analyses. *Compos Struct*. 2021;276:114548.
55. Yan G. A Bayesian approach for damage localization in plate-like structures using Lamb waves. *Smart Mater Struct*. 2013; 22(3):035012.
56. Wagner PR, Nagel J, Marelli S, Sudret B. *UQLab User Manual—Bayesian inference for model calibration and inverse problems, Report # UQLab-V1.4-113, Chair of Risk, Safety and Uncertainty Quantification*. ETH Zurich; 2021.
57. Kumar Y. The Rayleigh-Ritz method for linear dynamic, static and buckling behavior of beams, shells and plates: a literature review. *J Vib Control*. 2018;24(7):1205-1227.

How to cite this article: Marques D, Vandepitte D, Tita V. Sensitivity and uncertainty analysis for structural health monitoring with crack propagation under random loads: A numerical framework in the frequency domain. *Fatigue Fract Eng Mater Struct*. 2022;1-16. doi:10.1111/ffe.13853